Current-Induced Insulator-Metal Transition and Pattern Formation in an Organic Charge-Transfer Complex

R. Kumai,[1]* Y. Okimoto,[1] Y. Tokura[1,2]

Organic molecular Mott insulators, in which carriers are localized as a result of the electron correlation, showed nonlinear electric conduction upon application of a high electric field along the molecular stacking axis. The current-driven low-resistive state of potassium 7,7,8,8-tetracyanoquinodimethanane was stabilized down to 2 kelvin, where a metallic path was visible with a microscope. The current flow caused a stripe-like periodic phase-segregation into the carrier-rich and carrier-poor regions along the current path.

In many organic charge-transfer complexes, π electrons are localized on molecular sites as a result of the strong electron-electron repulsion interaction. In those compounds, the electrical resistance is usually high and displays a thermal activation type of behavior with a relatively large activation energy ($\geq$ 0.1 eV). Alkali-7,7,8,8-tetracyanoquinodimethane (TCNQ) (*1–3*) is a quasi–one-dimensional organic charge-transfer complex with segregated columns of alkali cation and TCNQ anion. In this salt one π electron is localized on the TCNQ site, forming an anion radical ($TCNQ^{-\bullet}$) (as in the Mott-Hubbard insulator) because of its fairly large on-site Coulomb repulsion as compared with the transfer energy between the adjacent TCNQ sites along the acceptor column. Alkali-TCNQ crystal undergoes a structural phase transition at critical temperature (T_c) (348 K for Na-TCNQ, 395 K for K-TCNQ, 381 K for Rb-TCNQ, and 210 K for Cs-TCNQ), and the $TCNQ^{-\bullet}$ stacks are dimerized below T_c (*4–6*). The magnetic susceptibility decreases rapidly below T_c because of the formation of magnetically inactive (singlet) TCNQ dimer. In this sense, the transition is viewed as a spin-Peierls transition (*7*, *8*). K-TCNQ investigated here is one such alkaline TCNQ and shows insulating behavior over the whole temperature region below and above T_c. Here we report that application of a high voltage or resultant current injection can induce a sort of dielectric breakdown in K-TCNQ crystal, resulting in a very large reduction of the sample resistance over the whole temperature region.

We prepared single crystals of K-TCNQ by the standard diffusion method using an H-shaped Pyrex cell (25 ml) in which TCNQ and potassium iodide (KI) were loaded at both ends and diffused in acetonitrile under an argon atmosphere at room temperature. Reddish-purple needles were obtained with a typical size of 10 by 2 by 2 mm^3, and the cell parameters estimated by a four-circle x-ray diffractometer were the same as those reported in the literature (*3*). We measured the current (I) versus voltage (V) curves on K-TCNQ single crystals with two-terminal electrodes of carbon paste by applying high-voltage pulses with a pulse duration of 200 ms. In the measurement circuit, a load resistor R_L (100 kilohm to ~2 megohm) was connected in series to prevent a sudden burst of current when the resistance changed. The measurements were made at various temperatures while keeping the sample in a continuous flow of cold helium gas.

The circuit, which included a crystal of K-TCNQ as a resistive element in series, showed nonlinear I-V characteristics when the current flowed along the TCNQ stacking axis (*a* axis; see the top diagram in Fig. 1 for a crystal structure). This behavior stems from the nonlinear electrical conduction of the K-TCNQ crystal itself. We calculated the current density (J) –electric field (E) characteristics for the K-TCNQ crystal (Fig. 1) from the observed I-V curves with respect to the two current directions ($I//a$ and $I//c$) at 280 K. In the case of current parallel to the *a* axis (stack axis), when the current density exceeds 0.08 A cm^{-2}, the J-E curve shows a negative differential-resistance feature, in accord with the one previously observed for Rb-TCNQ (*9*). (Without a load resistor R_L, the current burst would result in explosive an break-up of the crystal.) In contrast, the J-E curve for $I//c$ (that is, perpendicular to the stack axis) shows ohmic behavior up to 10^4 V cm^{-1}. This observation indicates that the resistive transition induced by current arises from the one-dimensional π-electron dynamics.

The temperature variation of the I-V curves (Fig. 2A) measured by applying pulsed voltage along the stack axis depends on the ratio of R_L to the low-field resistance of the sample. However, the J-E curves (Fig. 2B), which are reduced from the I-V curves, are nearly identical for several different samples at respective temperatures when a suitable R_L was connected in the circuit. The I-V curves show a hysteresis when the triangle-shape voltage is applied instead of pulse voltage. This hysteresis effect arises from the current bistability in the circuit, which contains a negative-differential-resistance element, whereas the J-E characteristics inherent to the crystal show no hysteresis. In the temporal response of the switching (Fig. 2C), when a pulsed electric field is applied, the current in the circuit rises up to 30% of the final value instantaneously within the resolution limit of the voltage source (= 1 ms). Then the current grows gradually and reaches a constant value after 200 ms. The latter slow process may be explained in terms of the growth of the conducting path volume, as evidenced by the direct observation under a microscope.

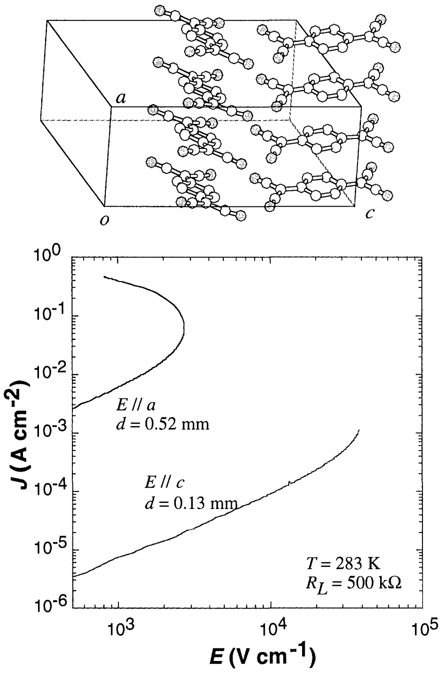

Fig. 1. Current density versus electric field (J-E) curves of a K-TCNQ crystal at 283 K with E parallel (//*a*) and perpendicular (//*c*) to the TCNQ-stacking axis (*a* axis). The respective values of J and E were derived from the current versus voltage (I-V) curves, that were measured for the circuit composed of the K-TCNQ crystal and the load resistor (R_L = 500 kilohm) in series. The relations used to calculate the J and E values are $J = I/S$ and $E = (V - IR_L)/d$, where S and d are the cross-sectional area and the electrode gap, respectively. The crystal structure of K-TCNQ is depicted at the top, where H and K atoms are omitted for clarity. TCNQ columns along the *a* axis are slightly dimerized below 381 K (*6*).

---

[1] Joint Research Center for Atom Technology (JRCAT), Tsukuba 305-0046, Japan. [2] Department of Applied Physics, University of Tokyo, Tokyo 113-0033, Japan.

*To whom correspondence should be addressed. E-mail: rkumai@jrcat.or.jp

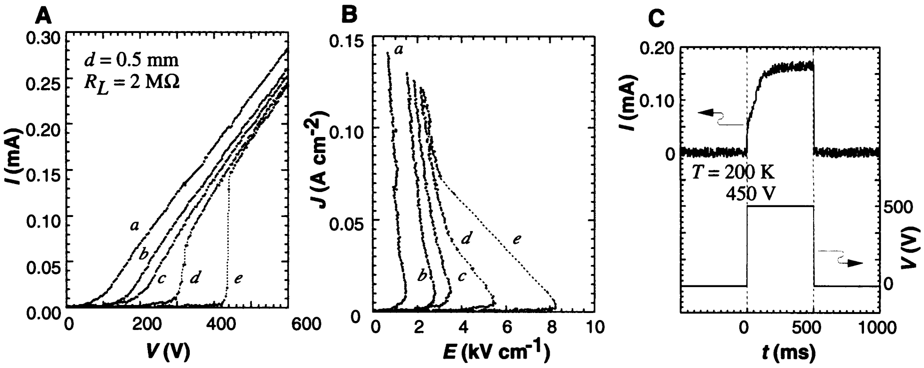

Fig. 2. (**A**) *I-V* characteristics (*I*//*a*) of the crystal at various temperatures (curve a, 300 K; curve b, 280 K; curve c, 230 K; curve d, 180 K, curve e, 180 K) with the circuit composed of the K-TCNQ crystal with the electrode gap (*d*) and the load resistor (R_L) in series. (**B**) *J-E* characteristics (*J*, *E*//*a*) of the crystal at the respective temperatures. (**C**) Temporal response of the current switching at 200 K measured with the use of a 450-V voltage pulse with a duration of 500 ms.

The temperature dependence of the resistance of the crystal, which was measured with constant R_L in the circuit by application of constant-voltage pulses, is shown in Fig. 3. When the voltage is low (V = 10 V or E = 192 V cm^{-1} at 300 K), the resistance of the crystal increases with decreasing temperature (with an activation energy of E_a = 0.2 eV) in the same manner as in the conventional small-constant-current (I = 1 μA) measurement (by the four-probe method, shown also in Fig. 3). Once the voltage of 100 V is applied (E = 1920 V cm^{-1} at 300 K), the resistance is decreased by an order of magnitude, but it abruptly jumps up to the original low-voltage value when the sample is cooled to 240 K. When the applied voltage is higher than 200 V, however, the resistance does not diverge with decreasing temperature even down to 2 K. This suggests that the low-resistive state or the conduction path generated by the current is metallic in nature. The nominal resistivity ρ under V = 500 V is still considerably large, ≈3 × 10^3 ohm cm, as the metallic one, but this should not be considered as a bulk value. As a possible origin of the current-induced conducting state, simple Joule heating can be excluded: In the heating scenario, the sample resistance under a 500-V pulse would be realized with the increase of the sample temperature above 600 K, as estimated by extrapolation of the temperature-dependent low-field resistance, but in this temperature region this organic compound would already have decomposed.

The electrically insulating state of the K-TCNQ crystal originates from the localization of each TCNQ π electron on the respective molecule by a strong on-site electron repulsion interaction (electron correlation effect). Therefore, the dielectric breakdown cannot be a single-electron event as observed in a conventional semiconductor (Zener effect), but must accompany a collapse of the electronic gap or otherwise collective carrier motion characteristic of an interacting one-dimensional electron system. The optically detected electronic gap is as large as 0.6 to 0.8 eV (*10*) and hence should be too large to be destroyed by such a relatively weak electric field as the one we used in the present experiment. Deviation from the exact half band-filling or the inevitable presence of low-density carriers might be responsible for the initiation of the dielectric breakdown in the weakest portions of the crystal.

We confirmed the generation of metallic paths by looking at the crystal under a microscope at room temperature with and without the application of an electric field, while monitoring its current switching behavior. Images for the sample surface projected on a cooled charge-couple device (CCD) camera are shown in Fig. 4. Without an electric field or before the current switching, the crystal surface between the carbon-paste electrodes appears homogeneously light-purple in color (Fig. 4A). Once the electric field was applied and the switching of resistive state initiated, a stripe pattern composed of alternating dark and bright purple regions emerged with a spacing of 3 to 14 μm (Fig. 4B). The stripe spacing appears to depend on the sample and the shape of the electrodes. In the sample shown in Fig. 4, the spacing becomes wider in going from the electrode edge toward the center region. The stripe region was observed only upon switching or in the low-resistive state and so can be regarded as a conductive path. The stripe edges are always almost perpendicular to the stack axis (*a* axis). The path width grows with applied voltage (Fig. 4C), and the process corresponds to the increase of current after the switching. Dynamic motion of the extension of the stripe-path width was confirmed under a microscope. The stripes are static in the steady-current state, and their periodicity along the stack axis does not change even with the change of electric field

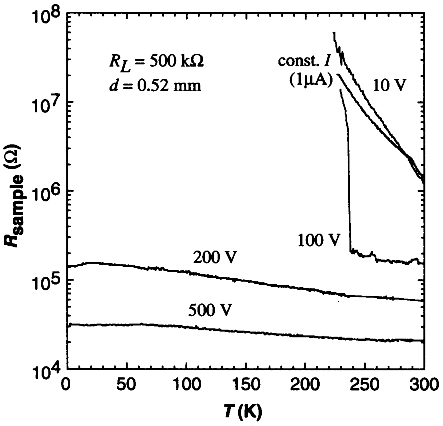

Fig. 3. Temperature dependence of resistance of a K-TCNQ crystal measured with various applied voltage pulses (200-ms duration). The sample resistance (R_{sample}) was estimated by the relation that R_{sample} = V/I − R_L. The low-field resistance of the same crystal measured by the conventional four-probe method with a low constant current (1 μA in the present case) is also shown. At V = 100 V, the crystal returns from a low-resistive to a high-resistive state around 200 K. However, the applied voltage of ~200 V is enough to maintain the low-resistive state or the metallic path down to the lowest temperature.

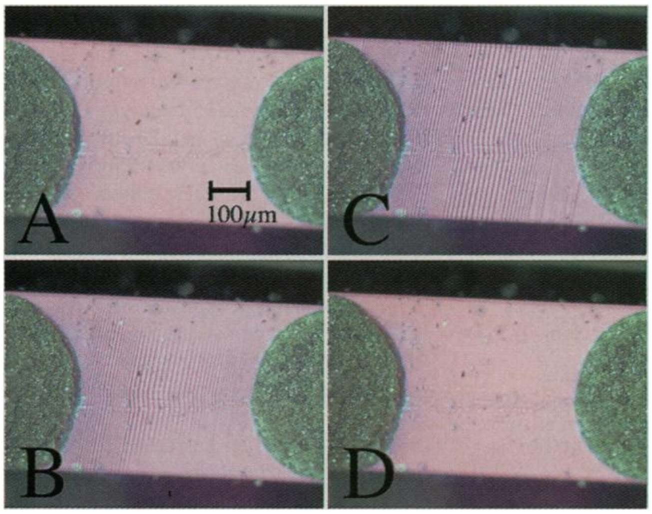

Fig. 4. Images of the sample surface projected on the CCD camera under a microscope at 290 K: (**A**) before the electric field was applied, (**B**) the low-resistive state with an electric current flow of 0.69 mA (an applied voltage V = 800 V in the whole circuit with a 1-megohm load resistor in series), (**C**) the low-resistive state with a higher current flow of 0.89 mA (V = 1000 V), and (**D**) after removal of the electric field.

(or current). The stripe pattern disappears again (Fig. 4D) when the electric field is removed and the crystal returns back to the high-resistive state. By the atomic force microscope measurement, the surface of the stripe pattern region was confirmed to be flat within 50 nm in height and hence the stripes are not due to groove-like strains. The dark stripe perhaps comes from metallic patches, because the metallic or nondimerized TCNQ stack gives rise to a lower reflectivity in the visible region (*11*). With use of the sensitivity of the totally symmetric (a_g) mode molecular vibration [CN stretching (ν_{CN}) of TCNQ] to the dimeric (Peierls-like) distortion (*10*), the microscopic infrared spectroscopy (*12*) has confirmed that the dimerization is much reduced in the current-flowing region accompanying the stripe pattern, but less so in the nonstripe region (corresponding to the crystal edge part in Fig. 4B). Such a current-path region characterized as the alternative dark and bright regions can be viewed as the periodic phase-segregation into carrier-rich (dark) and -poor (bright) regions.

This stripe pattern formation may originate from the long-range Coulomb repulsion interaction between the generated carrier-rich regions. A current-flowing state is a nonequilibrium state out of the scope of thermodynamics, yet the current-induced coexistence of the carrier-rich (high-conducting) and carrier-poor (low-conducting) regions may be viewed as a sort of phase segregation. This is perhaps inherent to the correlated electron system like K-TCNQ, where the hypothetical metallic state is, in the sense of free energy, adjacent to the Mott-insulating state in spite of a seemingly large charge-gap. A specifically large dielectric constant along the stacking axis can effectively screen the Coulomb interaction between the carrier-rich regions, producing such a stripe pattern running perpendicular to the stacking axis, as we observed. Thus, we consider the observed phenomenon as one example of the self-organization in nonequilibrium systems as widely seen in natural systems and extensively investigated for several decades (*13*, *14*). A distinct feature is, however, that the stripe pattern in the present case is composed of electronically different phases, namely metallic (nondimerized) and poorly conducting (dimerized) states.

References and Notes

1. Z. G. Soos, *Annu. Rev. Phys. Chem.* **25**, 121 (1974).
2. L. R. Melby *et al.*, *J. Am. Chem. Soc.* **84**, 3374 (1962).
3. J. Siemons, P. E. Bierstedt, R. G. Kepler, *J. Chem. Phys.* **39**, 3523 (1963).
4. J. G. Vegter, T. Hibma, T. Kommandeur, *Chem. Phys. Lett.* **3**, 427 (1969).
5. N. Sakai, I. Shirotani, S. Minomura, *Bull. Chem. Soc. Jpn.* **45**, 3321 (1972).
6. H. Terauchi, *Phys. Rev. B* **17**, 2446 (1978).
7. Y. Lepine, A. Caillé, V. Larochelle, *ibid.* **18**, 3585 (1978).
8. Y. Iwasa *et al.*, *ibid.* **39**, 10441 (1989).
9. N. Watanabe, Y. Iwasa, T. Koda, *ibid.* **44**, 11111 (1991).
10. H. Okamoto, Y. Tokura, T. Koda, *ibid.* **36**, 3858 (1987).
11. K. Yakushi *et al.*, *Chem. Phys. Lett.* **68**, 139 (1979).
12. Y. Okimoto, R. Kumai, Y. Tokura, unpublished data.
13. G. Nicolis and I. Prigogine, *Self-Organization in Nonequilibrium Systems* (Wiley, New York, 1977).
14. T. Fukui and N. Kawakami, *Phys. Rev. B* **58**, 16051 (1998).

15. We thank N. Nagaosa, N. Kawakami, and H. Fukuyama for enlightening discussions. We also thank M. Izumi for his help with atomic force microscope measurements. This work, partly supported by New Energy and Industrial Technology Development Organization, was performed at JRCAT under the joint research agreement between National Institute for Advanced Interdisciplinary Research and Angstrom Technology Partnership.

24 November 1998; accepted 19 April 1999

Enhanced Reactivity of Highly Vibrationally Excited Molecules on Metal Surfaces

H. Hou,[1] Y. Huang,[2] S. J. Gulding,[2] C. T. Rettner,[1] D. J. Auerbach,[1]* A. M. Wodtke[2]*

The chemical dynamics of highly vibrationally excited molecules have been studied by measuring the quantum state–resolved scattering probabilities of nitric oxide (NO) molecules on clean and oxygen-covered copper (111) surfaces, where the incident NO was prepared in single quantum states with vibrational energies of as much as 300 kilojoules per mole. The dependence of vibrationally elastic and inelastic scattering on oxygen coverage strongly suggests that highly excited NO (v = 13 and 15) reacts on clean copper (111) with a probability of 0.87 ± 0.05, more than three orders of magnitude greater than the reaction probability of ground-state NO. Vibrational promotion of surface chemistry on metals (up to near-unit reaction probability) is possible despite the expected efficient relaxation of vibrational energy at metal surfaces.

Excited states of molecules are often much more reactive than ground-state species, in part because internal energy can help overcome barriers to reaction. Reactions of electronically excited molecules have been studied extensively; indeed, most of the field of photochemistry involves such states. The preparation and study of vibrationally excited reactants has proven more difficult. In polyatomic molecules, vibrational excitation may not remain localized in particular vibrations, and even in diatomic species, such states can prove difficult to prepare in large fluxes (*1*). These difficulties are particularly great for highly vibrationally excited molecules, where the vibrational excitation is a substantial fraction of the bond energy. The motivation to study the chemistry of such species is strong. The atoms in such molecules have large kinetic energies, which may enhance reaction rates. Furthermore, large amplitude vibration can distort the molecular electronic wave function, altering physical and chemical properties.

A few measurements of the reactivity of highly vibrationally excited molecules in the gas phase have been performed (*2*) and have shown that such excitation can produce reaction cross sections approaching the gas kinetic limit. Studies of the interactions of vibrationally excited molecules with surfaces have been restricted to low-lying vibrational states, populated either thermally (*3*) or with optical excitation (*4*). The reaction probabilities observed, although strongly influenced by vibration, were low (10^{-2}).

Unlike gas-phase reactions, it has not been clear that increasing the reactant vibrational excitation for reactions at surfaces can ever yield high reactivity. Particularly for metal surfaces, vibrational relaxation is potentially an important competitive channel. Indeed, theory predicts that vibrational relaxation rates will increase with the vibrational energy of the initial state (*5*, *6*) and thus could effectively thwart attempts to reach large reaction probabilities by using highly vibrationally excited molecules.

We present an experimental method that can reveal the chemical dynamics of highly vibrationally excited molecules at solid surfaces. We illustrate our approach using the model system of NO molecules interacting with a Cu(111) surface, where we observe a thousandfold vibrational enhancement of surface reactivity. In contrast, neither reagent translational energy nor surface temperature has a strong effect on the reaction probability

---

[1] IBM Research Division, Almaden Research Center, San Jose, CA 95120, USA. [2] Department of Chemistry, University of California, Santa Barbara, CA 93106, USA.

*To whom correspondence should be addressed.